

## Physico-Chemical Characterization and Interfacial Electrochemical Properties of Nanoparticles of Anatase-TiO<sub>2</sub> Prepared by the Sol-Gel Method

**Ikram Daou, Rachid Chfaira, Omar Zegaoui\*, Zakaria Aouni and Hammou Ahlafi**

Laboratoire « Chimie-Biologie Appliquées à l'Environnement »; Equipe de recherche « Matériaux et Catalyse Appliqués »; Université Moulay Ismail ; Département de chimie; Faculté des Sciences; BP. 11201 Zitoun, Meknès, Maroc

**Abstract:** In this work, we prepared by the sol-gel method titanium dioxide nanoparticles having a large specific area ( $S_{\text{BET}} = 218 \text{ m}^2/\text{g}$ ). The isotherm of N<sub>2</sub> adsorption-desorption at 77K revealed that it concerns a mesoporous solid with a maximum pore diameter of 43 Å. The X-ray diffraction showed that the solid is constituted of the anatase phase. The transmission electron microscopy revealed us that the synthesized grains of TiO<sub>2</sub> are of nanometric sizes (diameter between 8 and 20 nm) and manifest under agglomerated shape. The study of its solubility in dispersing phase, by conductometric titrations, showed that the prepared solid is totally insoluble in all the domain of the studied pH. The measured inter-facial electrochemical properties, based on the isotherms of ionic adsorption and the conductometric titrations, are: the point of zero charge found equal to 6,2±0,1, the total number of sites of surface found equal to 5,8 OH/nm<sup>2</sup> and the nature of action of the dispersed phase on the dispersing phase which is found organizer of the structure of water. Besides, the difference of the ionization constants  $\Delta pK$  is found superior to 4 for all the adsorbed ions and the constants of surface complexation are independent from the nature of the adsorbed ion.

**Key words:** Nanoparticles, Anatase-TiO<sub>2</sub>, Sol-gel, Interfacial electrochemical properties.

### Introduction

Currently, the titanium dioxide (TiO<sub>2</sub>) under the form of nanoparticles appears to be the material of the future for the resolution of the environmental problems such the organic and mineral pollution of the water and the air and the storage of the energy because of its photo-catalytic and photo-electrochemical properties<sup>1-4</sup>. The titanium dioxide has various polymorphs such as rutile, anatase and brookite<sup>5,6</sup>, but the anatase and rutile are thermodynamically the most stable at low temperature. There are several methods that can be used to prepare nanoparticles of titanium dioxide<sup>7-14</sup>; however, the sol-gel method is the most widely used because of its simplicity and its reproducibility. The aim of this work is to prepare, characterize by physico-chemical methods and determine the interfacial electrochemical properties of TiO<sub>2</sub> nanoparticles having high specific surface area.

\*Corresponding author:

E-mail address: [zomar17@yahoo.fr](mailto:zomar17@yahoo.fr)

DOI: <http://dx.doi.org/10.13171/mjc.2.4.2013.28.07.17>

The physico-chemical characterization was made by Fourier Transformed Infra-Red Spectroscopy (FTIR), X-Ray Diffraction (XRD), Transmission Electron Microscopy (TEM) and N<sub>2</sub> sorption at 77K.

The determination of the inter-facial electrochemical properties of prepared TiO<sub>2</sub> was carried out at 298K by ionic adsorption measurements and conductometric titrations in the presence of different electrolytes alkali-halide type 1-1 and at different ionic strengths. These electrochemical properties are the state of insolubility of the dispersed phase in the dispersing phase, the pH at the point of zero charge (pH<sub>pzc</sub>), the total number of surface sites (Ns), the ionization and the complexing constants and the nature of action of the dispersed phase on the dispersing phase.

The novelty of this work lies in the development in our laboratory of experimental methods based on the conductometric titrations. These techniques aimed at the determination of the pzc and the study of the solubility of TiO<sub>2</sub> nanoparticles in dispersing phase.

## Experimental Section

### Preparation of nanoparticles

The TiO<sub>2</sub> nanoparticles were prepared by the sol-gel method by using as precursor the titanium(IV) isopropoxide [Ti(O-iPr)<sub>4</sub>] purchased from Sigma Aldrich (purity: 99,99 %). The precursor is dissolved in the isopropanol bought also at Sigma Aldrich (purity: 99,99 %). The mixture is maintained under constant stirring at room temperature. The pH of the mixture being 4,4 and the hydrolysis is made under constant agitation adding distilled water and respecting a molar ratio  $r = \frac{[H_2O]}{[Ti(O-iPr)_4]} = 100$ . The obtained mixture is passed in the centrifuge at 5000 rpm/min for 10 min to separate TiO<sub>2</sub>. Finally, the obtained solid is washed with distilled water, filtered under vacuum and dried overnight in an oven at 373K. The TiO<sub>2</sub> prepared was calcined at 673K during 3 hours prior to characterization.

### Characterization of nanoparticles

The FTIR spectra (400-4000 nm) of prepared solids were obtained using a spectrophotometer type JASCO 4100. Crystalline structures of the powders were characterized by X-ray diffraction with a X'PERT MPD\_PRO diffractometer using Cu K $\alpha$  radiation. The accelerating and the applied current were 45 kV and 40 mA respectively. The determination of the crystalline phases was carried out by applying the Bragg law where  $\lambda = 1,5406 \text{ \AA}$ . The size and morphology of as-prepared nanoparticles were determined by Transmission Electron Microscopy imaging (microscope Tecnai 12 from FEI Company). A Nitrogen sorption experiments were carried out at 77 K using a Micromeritics ASAP 2010 apparatus. The surface area was calculated according to Brunauer, Emmet and Teller (BET) in the P/P<sub>0</sub> range of 0,05 to 0,3 and the pore size distribution was determined according to Barrett, Joyner and Halenda (BJH) from desorption branch of the isotherms.

### Potentiometric and conductometric titrations

#### Experimental device

The used experimental device is common to the potentiometric and conductometric titrations and allows measuring a surface charge of a solid having a volume fraction of minimal specific area of 5 m<sup>2</sup>/g. It is constituted of the following: a thermostatic bath settled at 298K, of a unit containing the suspension to be studied, a ball of glass combined electrode,

of the conductivity measurement unit, of a pH-meter, of a conductometer, of a helix agitator activated by an engine, of a micro-burette and of nitrogen gas entrance to chase away the atmospheric carbon dioxide from the measurement unit.

It is important to indicate that before every potentiometric or conductometric titration, it is necessary to leave the solid in dispersing phase age for approximately 20 hours. This time represents the necessary duration for the ionic exchange, characterizing the experimental parameter pH, between both dispersed and dispersing phases.

The used salts in this work are NaCl (purity: 99,9 %), KCl (purity: 99,9 %), NaF (purity: 99,5 %), KI (purity: 99,5 %) and LiCl (purity: 99,9 %). They are supplied by the Sigma Aldrich Company.

The used water is distilled and passed on a column of mixed resin. Its specific conductivity at the column exit is of  $0,510^{-6}$  ( $\Omega^{-1} \cdot \text{cm}^{-1}$ ).

### Principle of determining the surface charge

The surface charge of metallic oxides such as  $\text{TiO}_2$ , results from the uneven ions adsorption determining the potential  $\text{H}^+$  and  $\text{OH}^-$ <sup>15</sup>. The experimental measures of this charge are obtained by the potentiometric titrations of the solid suspensions prepared in the presence of a known constant concentration in electrolyte<sup>16</sup>.

## Results and Discussion

### FTIR Spectroscopy

The FTIR spectrum of  $\text{TiO}_2$  (**Figure 1A**) shows a broad band between 420 and 750  $\text{cm}^{-1}$ . As displayed in **Figure 1B** (inserted), it is due to several bands overlapping and which are attributed to different modes of vibration of  $\text{Ti-O}$ <sup>14,17-22</sup>. The bands at 420  $\text{cm}^{-1}$  and 450  $\text{cm}^{-1}$  are related to the vibration of  $\text{Ti=O}$  and the stretching vibration of  $\text{Ti-O}$  in the anatase, respectively. The stretching vibration of  $\text{Ti-O-Ti}$  group appears at 544  $\text{cm}^{-1}$  and the vibration at 629  $\text{cm}^{-1}$  is probably associated to the vibrations of  $\text{TiO}_6$  polyhedron. The shoulder at 839  $\text{cm}^{-1}$  can be linked to the vibration of the anatase  $\text{TiO}_2$ .

The spectrum also shows the presence of the other bands of low intensities located at 1387 and 1620  $\text{cm}^{-1}$ . The band at 1387  $\text{cm}^{-1}$  can be attributed to the symmetric stretching vibration of  $\text{CO}_2$  contained in the ambient air or to C-H deformation. The band at 1620  $\text{cm}^{-1}$  is attributed to the bending vibration of the adsorbed  $\text{H}_2\text{O}$  on the surface of the solid. We also note the presence of a broad absorption band between 3000 et 3600  $\text{cm}^{-1}$  (centred towards 3400  $\text{cm}^{-1}$ ) assigned to the stretching vibration of  $\text{H}_2\text{O}$  adsorbed on the surface of the solid<sup>19,23,24</sup>.

### X-Ray Diffraction

The XRD pattern of the prepared nanoparticles of  $\text{TiO}_2$  and calcined at 673K for 3 hours is given in **Figure 2**. It shows that the solid crystallizes in the anatase phase (all peaks have been indexed in the anatase phase).

### Transmission Electronic Microscopy

The TEM micrograph of the  $\text{TiO}_2$  nanoparticles (**Figure 3**) shows that the solid consists of highly agglomerated fine particles which have a homogeneous shape. The size of the individual particles is between 8 and 20 nm.

### Nitrogen adsorption/desorption isotherm at 77K

**Figure 4A** presents the nitrogen adsorption/desorption isotherm at 77K obtained for a prepared TiO<sub>2</sub> and calcined at 673K for 3 hours. The obtained isotherm is according to the IUPAC classification of type IV characteristic of mesoporous solids presenting a loop of hysteresis of type H2<sup>25</sup>. This hysteresis is characteristic of porous solids for which the size distribution and shape of the pores are not uniform.

The calculated specific area, using the BET method<sup>25</sup>, is of 218 m<sup>2</sup>/g. The pores size distribution was obtained using the BJH method from the desorption isotherm (**Figure 4B**). It shows that the diameters of pores vary between 30 and 50 Å with a maximum distribution towards 43 Å, indicating the presence of mesopores.

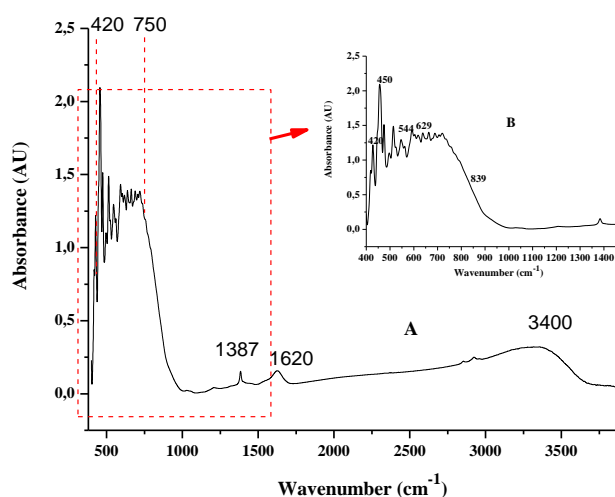


**Figure 1.** FTIR absorption spectra of TiO<sub>2</sub> nanoparticles

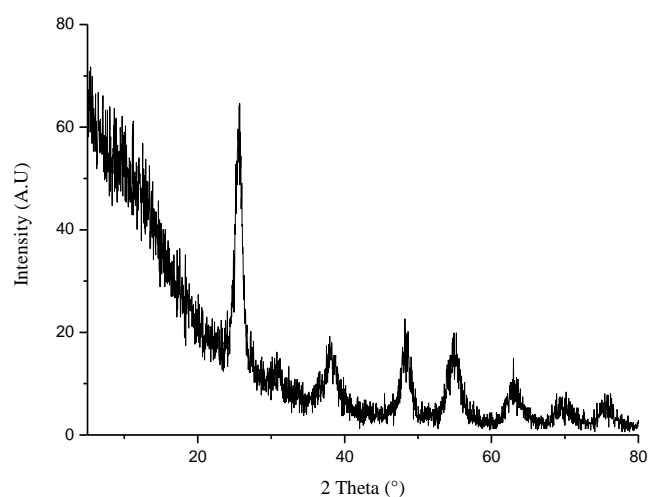


**Figure 2.** XRD spectrum of TiO<sub>2</sub> nanoparticles prepared and calcined at 673K for 3 hours

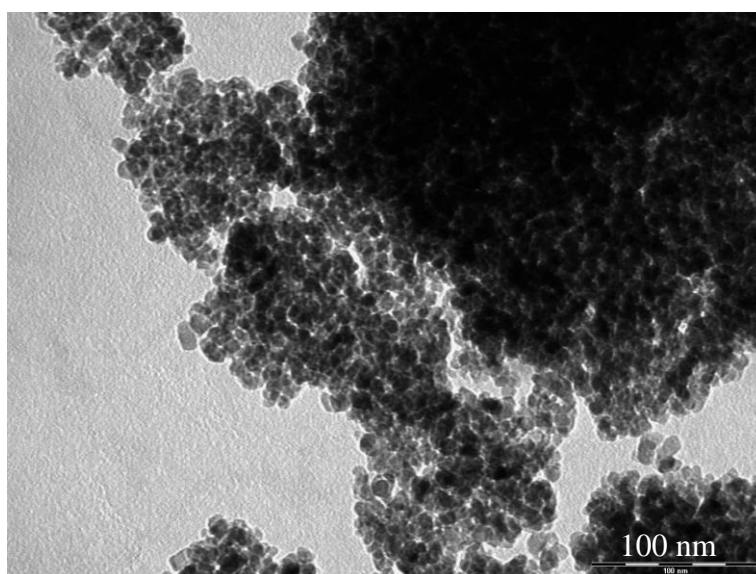


**Figure 3.** TEM micrograph of TiO<sub>2</sub> nanoparticles

### Solubility of TiO<sub>2</sub> powder prepared in dispersing phase

We studied the solubility of TiO<sub>2</sub> nanoparticles in aqueous phase at a given ionic force and under the same operating conditions of surface charge measurements to determine de pH range where the TiO<sub>2</sub> nanoparticles are in a colloidal state or in ideal insolubility.

The principle of this study is based on the comparison of the conductometric titrations curves in absence (white titration) and in presence of the studied solid. At a given pH, the difference of specific conductivity between both conductometric titrations curves corresponds to the conductivity brought by the soluble ionic species in solution deriving from the solubility of solid nanoparticles studied in aqueous phase.

**Figure 5** for example, shows the conductometric titrations curves obtained in absence and presence of the TiO<sub>2</sub> nanoparticles, in presence of LiCl at 10<sup>-3</sup> mol/L. We notice that both conductometric titrations curves coincide perfectly translating a colloidal state or perfect insolubility of the solid in all the domain of studied pH. A similar behaviour was observed in the presence of the other studied salts.

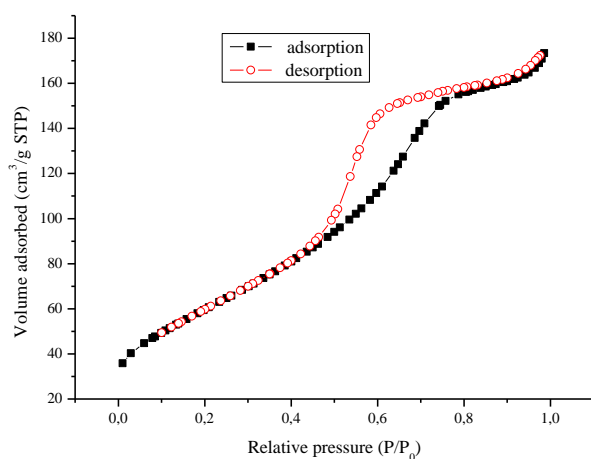


**Figure 4A.** Nitrogen adsorption/desorption isotherm at 77K

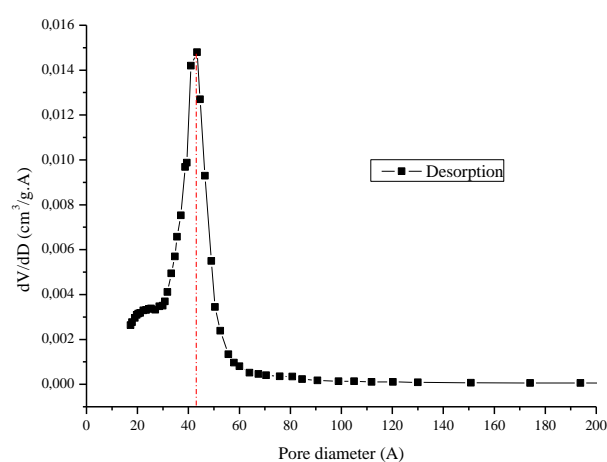


**Figure 4B.** BJH pores size distribution of nanoparticles of TiO<sub>2</sub>

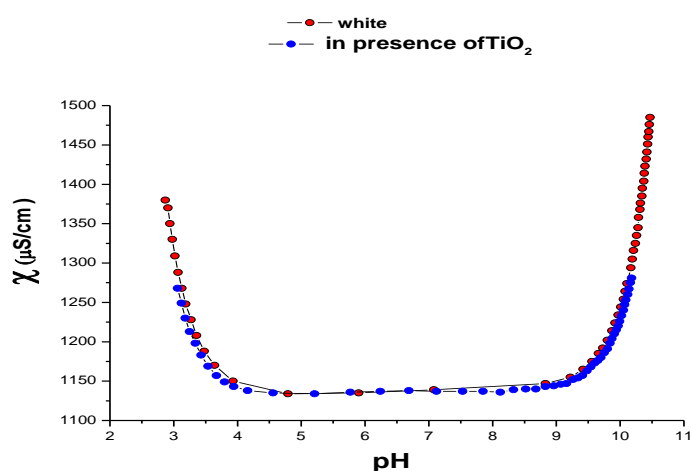


**Figure 5.** Specific conductivity curves in the absence (white titration) and in the presence of the TiO<sub>2</sub> nanoparticles prepared according to the pH of the salty aqueous suspension.

## Electrochemical properties of the interface TiO<sub>2</sub> solid/dispersing phase

### The point of zero charge (pzc)

The experimental determination of the pzc of a colloidal suspension can be made by several methods. If the potentiometric titrations are carried out in function of pH and salt concentration, the most used experimental approach is when the potentiometric curves intersect at a point. This point corresponds to the point of zero charge<sup>26,27</sup>.

In this work, we present a new experimental method for the determination of the pzc based on the conductometric titrations. As for metallic oxides the surface charge results from the uneven ions adsorption determining the potential H<sup>+</sup> and OH<sup>-</sup>, this method consists in following the consumption of these ions by various sites of surface.

The principle of this method consists in realizing conductometric titrations in absence and in presence of the solid at various ionic forces. The curves representing the difference of specific conductivity between those in absence (white titrations) and in presence of the solid according to the pH of the colloidal suspension and also according to the concentration of salt cross at a unique point which is the pzc.

Generally, in absence of specific adsorption, the net point of zero charge corresponds to the intersection of the isotherms of charge adsorption of measured surface at various ionic forces. **Figure 6A** shows the surface charge density variation of the titanium oxide prepared according to the pH and to the ionic force of the electrolyte KCl.

We clearly notice, that these surface charge curves cross at a unique point which is the pH at the pzc. For the titanium dioxide nanoparticles in the presence of a non specifically adsorbed electrolyte such as KCl, NaCl or KI, the measured value of the pH<sub>pzc</sub> is 6,2±0,1. In pH above this point, the studied solid nanoparticles are negatively charged while at pH less than the pH<sub>pzc</sub>, nanoparticles are positively charged.

The exploitation of the curves of the conductometric titrations in absence and in presence of the solid, led us to develop an original method of determination of the point of zero charge of a colloidal suspension. **Figure 6B** shows the application of this new technique of determination of the point of zero charge to the TiO<sub>2</sub> studied in presence of LiCl electrolyte.

We notice that the curve  $\Delta\chi$  according to the measured pH at ionic force equals to 10<sup>-2</sup> M, takes a form that is constituted of two branches with the tangents cross at a unique point which is the pH<sub>pzc</sub>. The found value equals 6,2±0,1 which is similar to that measured when applying the potentiometric titrations technique.

The validity of this new method is confirmed by its application on another standard TiO<sub>2</sub>, with different surface area (S<sub>BET</sub> = 8 m<sup>2</sup>/g), marketed by Sigma-Aldrich Company. **Figure 7A** shows the difference's variation of the specific conductivity ( $\Delta\chi = \chi_{\text{blanc}} - \chi_{\text{solide}}$ ) according to the pH and the concentration of LiCl in the solution.

We notice that these curves measured at various ionic forces are all formed by two branches which meet at a unique point which is the point of zero charge equal to 6,7±0,1. This measured value for TiO<sub>2</sub> commercial in the presence of the electrolyte LiCl is similar to that found by the potentiometric titrations method (**Figure 7B**).

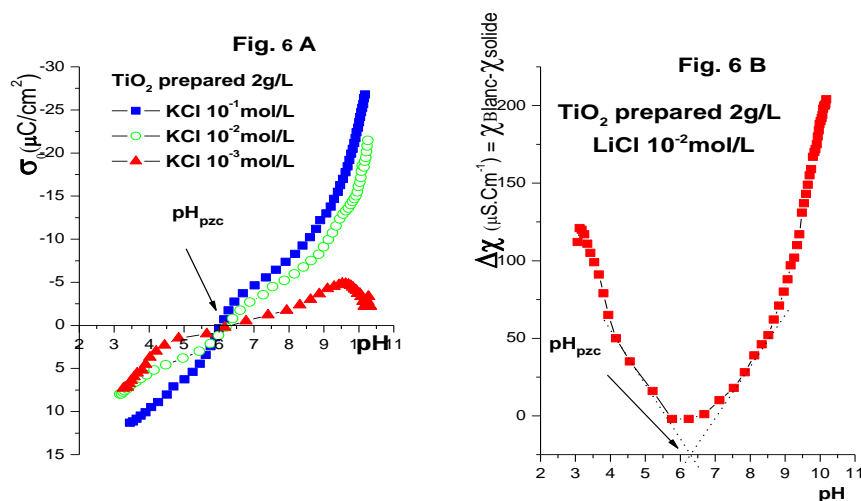


**Figure 6.** Determination of the  $\text{pH}_{\text{pzc}}$  of  $\text{TiO}_2$  nanoparticles prepared from potentiometric (A) and conductimetric (B) titrations

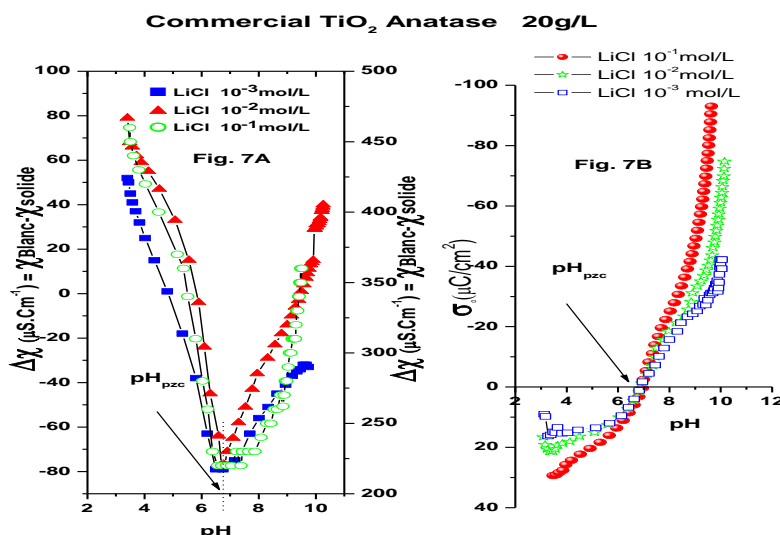


**Figure 7.** Determination of the  $\text{pH}_{\text{pzc}}$  of the commercial  $\text{TiO}_2$  from the conductometric (A) and potentiometric (B) titrations

### Nature of action of the dispersed phase on the dispersing phase

The knowledge of the nature of action of the dispersed phase on the dispersing phase is essential in the study of the stability of a colloidal suspension. In fact, the presence of a permanent hydration layer on the surface of particles increases considerably the stability of the studied hydrosol<sup>17</sup>.

The ionic adsorption on the prepared titanium oxide is studied in pH superior to the pzc in the presence of alkaline cations  $\text{Li}^+$ ,  $\text{Na}^+$  and  $\text{K}^+$  and with pH inferior to the pzc in the presence of halides anions  $\text{F}^-$ ,  $\text{Cl}^-$  and  $\text{I}^-$ .

**Figure 8A** shows the sequence of ionic adsorption observed on the anatase  $\text{TiO}_2$  solid prepared in the domain of pH superior to the pzc with ionic force  $10^{-3}$  mol/L.

In a given pH, the more an ion is adsorbed on a surface the bigger the developed surface charge density becomes. On the basis of this definition, we can say that the sequence of adsorption observed on the studied solid with  $\text{pH} > \text{pH}_{\text{pzc}}$  is the following:  $\text{Li}^+ > \text{Na}^+ > \text{K}^+$ .

The same sequence of ionic adsorption is observed at ionic forces  $10^{-2}$  and  $10^{-1}$  mol/L. At pH inferior to the pzc, the **Figure 8B** shows the sequence of ionic adsorption observed on the TiO<sub>2</sub> oxide prepared at various ionic forces:  $F^- > Cl^- > I^-$ . In other words, the ion  $F^-$  is more adsorbed than  $Cl^-$  which is also more adsorbed than the ion  $I^-$ . It is more practical to carry the charge of surface  $\sigma_0$  according to  $\Delta pH$  in order to eliminate the effect of the specific adsorption of the fluorine ion strongly adsorbed.

The interpretation of the sequence of ionic adsorption observed on the studied oxide requires the study of respective interactions between the surface of solids and water, between the ions and the surface, and between the ions and water. Frank, Evans, Gurney and Gierst's theoretical models<sup>28,29</sup> allow the study of all these interactions. The following important conclusion is drawn from the combination of these theoretical models: an ion is particularly adsorbed to an interface that its action on the structure of water is similar to the interface.

As the ion  $Li^+$ , which is the most adsorbed on the negative surface, and the ion  $F^-$ , which is the most adsorbed on the positive surface, are organizing ions of the structure of the water<sup>30</sup> then the TiO<sub>2</sub> nanoparticles prepared act in solution as organizer of the structure of the water.

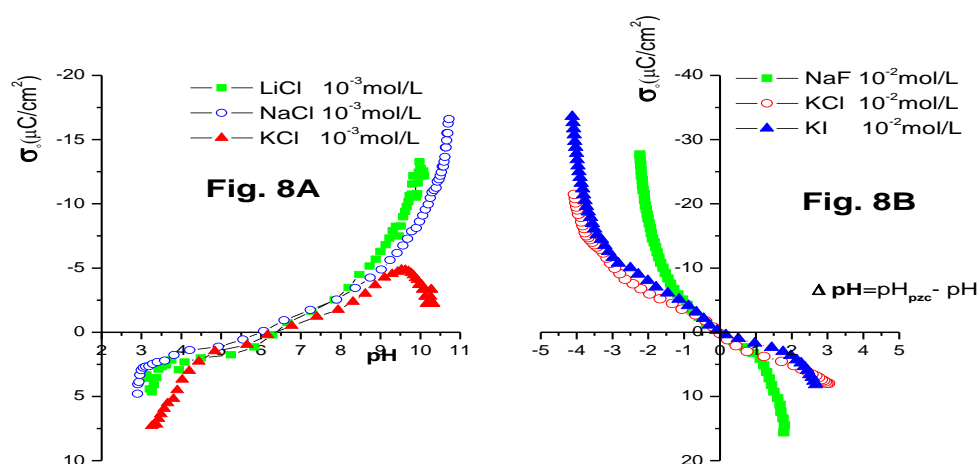


**Figure 8.** Sequence of ionic adsorption observed on the prepared oxide TiO<sub>2</sub>. (A) with  $pH > pH_{pzc}$  and (B) with  $pH < pH_{pzc}$

### Total number of surface sites $N_s$

The determination's principle of  $N_s$  by application of Stumm, Huang and Jenkins's graphic extrapolation technique<sup>31,32</sup> is based on the choice of the electrolytes which depends on the nature of the solid action on the dispersing phase.

For the organizing oxides of the structure of the water, the case of the studied TiO<sub>2</sub> oxide, it is necessary to choose for the positive surface of the solid, the graphic extrapolation of the curve  $\frac{1}{[H_s^+]}$  in function  $(\frac{1}{\sigma_0})$  corresponding to the most electronegative anion of the periodic table, which is the anion  $F^-$ , and which is the most organizing and most adsorbed. For the negative surface of the solid, it is necessary to choose the graphic extrapolation of the curve  $[H_s^+]$  in function  $(-\frac{1}{\sigma_0})$  corresponding to the most electropositive alkaline cation  $Li^+$  of the periodic table and which is the most adsorbed on the studied solid.

The graphic extrapolation corresponding to the anion  $F^-$  allows the determination of number of positive sites  $N_s^+$  and the one corresponding to the ion  $Li^+$  gives the number of negative sites  $N_s^-$ . The total number of sites is  $N_s = N_s^+ + N_s^-$



The determination's principle of the total density of sites of surface for the disorganizing oxides is opposite to that of the organizing surfaces.

**Figures 9A** and **9B** show the obtained straights and their corresponding equations respectively in the adsorption of the ion  $F^-$  and the ion  $Li^+$ . The calculated value of  $N_s^+$  is in the order of  $43,22 \mu C/cm^2$  and that of  $N_s^-$  is in the order of  $50 \mu C/cm^2$ . The value of the total density of sites of surfaces  $N_s$  of the solid prepared  $TiO_2$  is:

$$N_s = N_s^+ + N_s^- = 93 \mu C/cm^2$$

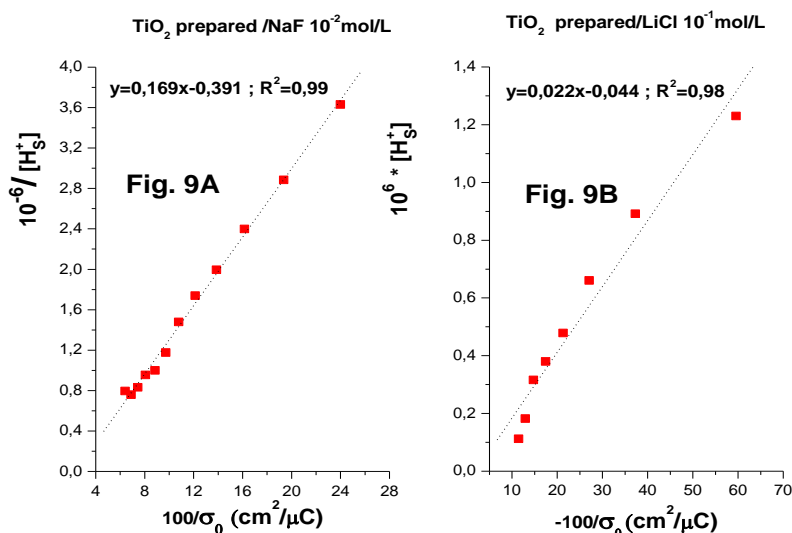


**Figure 9.** Curves of determination of the total density of sites of surface  $N_s$  of  $TiO_2$  oxide prepared by the graphic extrapolation method.

The found value for  $N_s$  in  $\mu C/cm^2$  does not exactly translate the maximal exchange capacity adsorbat-adsorbing of the prepared titanium oxide. It is necessary to convert  $N_s$  in number of OH group per  $nm^2$  called sites density by unit of surface, and noted  $D_s$ <sup>33</sup>.

$$D_s = \frac{\text{nombre of surface sites}}{\text{unit of surface}} = \frac{n_s \cdot N_{AV}}{A \cdot m_s}$$

A: the solid specific surface.

$m_s$ : mass of the studied solid.

$n_s$ : equivalent number of mole of titrated sites

$N_{AV}$ : Avogadro number

$$D_s = 6,24 \cdot 10^{-2} \cdot N_s \text{ (OH/nm}^2\text{)} = 5,8 \text{ (OH/nm}^2\text{)}$$

### Constants of ionization and of complexation of the prepared $TiO_2$ nanoparticles

The determination of the constants of ionization and of complexation by the application the site-binding model of Davis, James and Leckie<sup>34,35</sup>, is essentially based on the following equations:

### \* Ionization constants

- With pH below the  $pH_{pzc}$  where the particles surface is positively charged

$$pK_{int}^+ = pH + \log\left(\frac{\alpha^+}{1-\alpha^+}\right) + \frac{e\psi_0}{2,303kT} - \log\left\{1 + K_{int}^{An}[An^-] \cdot \exp\left(\frac{e\psi_\beta}{2,303kT}\right)\right\}$$

$$pK_{int}^+ = pQ^+ + \frac{e\psi_0}{2,303kT} - \log\left\{1 + K_{int}^{An}[An^-] \cdot \exp\left(\frac{e\psi_\beta}{2,303kT}\right)\right\}$$

If we take  $pQ^+$  according to  $10^{\alpha^+ + \sqrt{C_s}}$ , the constant  $pK_{int}^+$  can be determined by a double graphic extrapolation until  $\alpha^+ = 0$  and  $C_s = 0$  mol/L.

- At pH above the  $pH_{pzc}$  where the particles surface is negatively charged

$$pK_{int}^- = pH - \log\left(\frac{\alpha^-}{1-\alpha^-}\right) + \frac{e\psi_0}{2,303kT} + \log\left\{1 + K_{int}^{Ca}[Ca^+] \cdot \exp\left(-\frac{e\psi_\beta}{2,303kT}\right)\right\}$$

$$pK_{int}^- = pQ^- + \frac{e\psi_0}{2,303kT} + \log\left\{1 + K_{int}^{Ca}[Ca^+] \cdot \exp\left(-\frac{e\psi_\beta}{2,303kT}\right)\right\}$$

If we take  $pQ^-$  according to  $10^{\alpha^- + \sqrt{C_s}}$ , the constant  $pK_{int}^-$  can be determined by a double graphic extrapolation until  $\alpha^- = 0$  and  $C_s = 0$  mol/L.

The values of constants  $pK_{int}^-$  and  $pK_{int}^+$  of the prepared  $TiO_2$  solid in the presence of studied electrolytes, determined by D.J.L's double extrapolation graphic method<sup>34,35</sup>, are summarized in the table 1.

**Table 1.** The ionizations constants values  $pK_{int}^-$  and  $pK_{int}^+$  of the prepared  $TiO_2$  determined by the double extrapolation graphic method

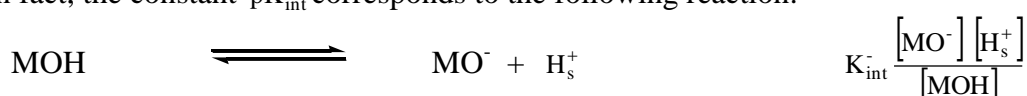
| Nature of electrolyte                     | LiCl | NaCl | KCl | KI  |
|---|------|------|-----|-----|
| $pK_{int}^-$                              | 8,4  | 8,5  | 9   | 8,4 |
| $pK_{int}^+$                              | 3,7  | 3,7  | 3,5 | 3,3 |
| $pH_{pzc} = 1/2(pK_{int}^+ + pK_{int}^-)$ | 6,1  | 6,1  | 6,2 | 5,9 |
| $\Delta pK = pK_{int}^- - pK_{int}^+$     | 4,7  | 4,8  | 5,5 | 5,1 |

### - Interpretation of the $pK_{int}^-$ values

We notice for the values related to the adsorbed cations  $Li^+$ ,  $Na^+$  of the NaCl and  $K^+$  of KCl electrolyte:  $pK_{int}^-(Li^+) = 8,4 < pK_{int}^-(Na^+) = 8,5 < pK_{int}^-(K^+) = 9$

The explanation of this order of constants  $pK_{int}^-$ , requires the intervention of the ionic adsorption sequence observed on the prepared  $TiO_2$  solid with pH superior to  $pH_{pzc}$ .

In fact, the constant  $pK_{int}^-$  corresponds to the following reaction:



The more an ion is adsorbed on a solid the bigger the density of charge or the concentration of  $[MO^-]$  becomes. In that case, the value of  $K_{int}^-$  is big and consequently  $pK_{int}^-$  is small.

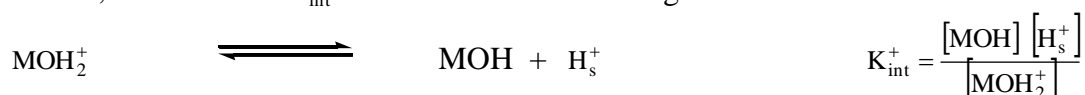
As the sequence of ionic adsorption observed on the studied solid is in the order  $\text{Li}^+ > \text{Na}^+ > \text{K}^+$ , we must expect the following order of  $\text{pK}_{\text{int}}^-$ :  $\text{pK}_{\text{int}}^-(\text{Li}^+) < \text{pK}_{\text{int}}^-(\text{Na}^+) < \text{pK}_{\text{int}}^-(\text{K}^+)$  Which is in accordance with the found values of  $\text{pK}_{\text{int}}^-$  of the prepared  $\text{TiO}_2$  nanoparticles.

#### - Interpretation of the $\text{pK}_{\text{int}}^+$ values

Concerning the  $\text{pK}_{\text{int}}^+$  values related to the adsorbed anions at the surface positively charged with the prepared  $\text{TiO}_2$  nanoparticles, the comparison can only be made between the  $\text{pK}_{\text{int}}^+$  related to the anion  $\text{Cl}^-$  of the salt  $\text{KCl}$  and the anion  $\text{I}^-$  of the salt  $\text{KI}$ :

$$\text{pK}_{\text{int}}^+(\text{Cl}^-) > \text{pK}_{\text{int}}^+(\text{I}^-)$$

However, the constant  $\text{K}_{\text{int}}^+$  is related to the following reaction:



The more an anion is adsorbed on the surface, the bigger the concentration of the positive sites  $[\text{MOH}_2^+]$ , and consequently  $\sigma_0$  is big. In that case,  $\text{K}_{\text{int}}^+$  is small and consequently  $\text{pK}_{\text{int}}^+$  is big. As the sequence of ionic adsorption observed on the studied  $\text{TiO}_2$  solid is in the order:  $\text{Cl}^- > \text{I}^-$ . Therefore, we have to expect that:  $\text{pK}_{\text{int}}^+(\text{Cl}^-) > \text{pK}_{\text{int}}^+(\text{I}^-)$ ; which is in agreement with the obtained experimental results.

The ionization constants values  $\text{pK}_{\text{int}}^-$  and  $\text{pK}_{\text{int}}^+$  obtained for the prepared  $\text{TiO}_2$  can be interpreted as follows:

- The comparison of the measured experimental value of the intrinsic pzc of the solid and the one due to the specific adsorption with the value calculated from the expression of  $\text{pH}_{\text{pzc}} = 1/2(\text{pK}_{\text{int}}^+ + \text{pK}_{\text{int}}^-)$ .

- The comparison of the values of  $\Delta\text{pK}$  calculated with those of the literature corresponding to organizing oxides<sup>35,36</sup>.  $\Delta\text{pK}$  is a surface property intrinsic to every colloidal suspension.

We notice that the values of pzc measured in the presence of  $\text{LiCl}$ ,  $\text{NaCl}$ ,  $\text{KCl}$  and  $\text{KI}$  salts are the same as those calculated from the ionization constants. It is thus important to indicate that the double extrapolation graphic method used to determine the ionization constants, also detects the specific adsorption which occurs in the case of the ion adsorption  $\text{Li}^+$ .

We also notice that the  $\Delta\text{pK}$  values related to all the adsorbed ions on the prepared  $\text{TiO}_2$  solid are superior to the value 4. This is in accordance with several works<sup>37-39</sup> stating that the oxides having a relatively weak density of sites  $N_s$ , as in the case of the studied  $\text{TiO}_2$  nanoparticles, are characterized by a high  $\Delta\text{pK}$ , superior to 4.

#### \* Complexation Constants

- With  $\text{pH}$  inferior to  $\text{pH}_{\text{pzc}}$  where the surface of particles is positively charged

$$\begin{aligned} \text{p}^* \text{K}_{\text{int}}^{\text{An}} &= \text{pK}_{\text{int}}^+ - \text{pK}_{\text{int}}^{\text{An}} = \text{pH} + \log\left(\frac{\alpha^+}{1 - \alpha^+}\right) - \log[\text{An}^-] + \frac{e(\psi_0 - \psi_\beta)}{2,303kT} \\ &= \text{p}^* \text{Q}^{\text{An}} + \frac{e(\psi_0 - \psi_\beta)}{2,303kT} \end{aligned}$$

If we take  $\text{p}^* \text{Q}^{\text{An}}$  according to  $10\alpha^+ - \log C_s$  using also the data of surface charges corresponding to high ionic forces  $10^{-2}$  and  $10^{-1}$  M, the constant of complexation  $\text{p}^* \text{K}_{\text{int}}^{\text{An}}$  can be determined by a double graphic extrapolation until  $\alpha^+ = 0$  and  $C_s = 1 \text{ mol/L}$ .

- With pH superior to  $pH_{pzc}$  where the surface of particles is negatively charged:

$$\begin{aligned} p^*K_{int}^{Ca} &= pK_{int}^+ + pK_{int}^{Ca} = pH - \log\left(\frac{\alpha^-}{1-\alpha^-}\right) + \log[Ca^+] + \frac{e(\psi_0 - \psi_\beta)}{2,303kT} \\ &= p^*Q^{Ca} + \frac{e(\psi_0 - \psi_\beta)}{2,303kT} \end{aligned}$$

If we  $p^*Q^{Ca}$  according to  $10\alpha^- - \log C_s$  using also the data of surface charges corresponding to high ionic forces  $10^{-2}$  and  $10^{-1}$  M, the constant of complexation  $p^*K_{int}^{Ca}$  can be determined by a double graphic extrapolation until  $\alpha^+ = 0$  and  $C_s = 1$  mol/L.

To determine the intrinsic constants of complexation, Davis-James and Leckie<sup>34,35</sup> were based on the approximation that at high concentrations of electrolyte (strictly superior to  $10^{-3}$  mol/L), the oxides surface charge is essentially due to the formation of the complexes on the surface. For this reason, we were limited only to the data of surface charge corresponding to the ionic forces  $10^{-2}$  and  $10^{-1}$  mol/L of the studied electrolyte.

**Table 2** summarizes the values of the constants  $p^*K_{int}^{Ca}$  and  $p^*K_{int}^{An}$  determined by a double graphic extrapolation until  $\alpha^+ = 0$  or  $\alpha^- = 0$  and  $C_s = 1$  mol/L for all the studied electrolytes.

**Table 2.** Complexation constants' values  $p^*K_{int}^{Ca}$  and  $p^*K_{int}^{An}$  of the prepared  $TiO_2$  oxide determined by the double graphic extrapolation method.

| Nature of electrolyte                               | LiCl | NaCl | KCl  | KI  |
|---|------|------|------|-----|
| $p^*K_{int}^{Ca}$                                   | 8    | 8,2  | 8,5  | 8,3 |
| $p^*K_{int}^{An}$                                   | 3,7  | 3,7  | 3,7  | 3   |
| $\log(K_{int}^{Ca}) = pK_{int}^- - p^*K_{int}^{Ca}$ | 0,4  | 0,3  | 0,50 | 0,1 |
| $\log(K_{int}^{An}) = p^*K_{int}^{An} - pK_{int}^+$ | 0    | 0    | 0,2  | 0,3 |

Table 2 also contains the values of  $K_{int}^{Ca}$  and  $K_{int}^{An}$  which really translate the phenomenon of complexation at the particles' surface. These values are deduced from those of the ionization constants  $pK_{int}^-$  and  $pK_{int}^+$  and complexation constants  $p^*K_{int}^{An}$  and  $p^*K_{int}^{Ca}$ .

Constants  $p^*K_{int}^{An}$  and  $p^*K_{int}^{Ca}$  have no physical sense, and it is the constants  $K_{int}^{Ca}$  and  $K_{int}^{An}$  that really translate the phenomenon of complexation which occurs at the surface of the studied solid.

The comparison of the constants values  $\log(K_{int}^{Ca})$  for studied electrolytes LiCl, NaCl, KCl and KI shown in table 2, shows clearly similar values. The same remark can be made for the  $\log(K_{int}^{An})$  values.

The found result shows clearly that for the prepared  $TiO_2$  solid, the phenomenon of complexation on a positive or negative surface is not specific in a given ion, but is of a purely electrostatic nature.

## Conclusion

In this work, we prepared mesoporous titanium dioxide nanoparticles with a large specific area ( $S_{\text{BET}} = 218 \text{ m}^2/\text{g}$ ). The maximal diameter of pores is 43 Å. The X-rays diffraction reveals that the solid is constituted of the anatase phase. The TEM observation revealed to us that the synthesized  $\text{TiO}_2$  is formed of agglomeration of nanoparticles. The study of its solubility in dispersing phase, by conductometric titrations, showed that the prepared solid is totally insoluble in the range of pH studied.

The interfacial electrochemical properties of  $\text{TiO}_2$  oxide are mainly the  $\text{pH}_{\text{pzc}}$ . It can be determined both by the classical method of the potentiometric titrations and by a method developed in this work based on the conductometric titrations.

The value of the intrinsic  $\text{pH}_{\text{pzc}}$  measured by both methods is the same and it is equal to  $6,2 \pm 0,1$ . The total number of sites of surface Ns, determined by extrapolation graphic method, found equal to  $5,8 \text{ OH}/\text{nm}^2$ .

The study of the ionic adsorption sequence at different ionic forces showed a structuring action nature of the prepared solid particles on the dispersing phase. The application of triple layer model on the realized surface charge density measures gave a difference of the ionization constants  $\Delta\text{pK}$  superior to 4 for all the adsorbed ions, characteristics of organizing oxides, and the constants of surface complexation are independent from the nature of the adsorbed ion.

## References

1. Y.-F. Chen, Ch-Y. Lee, M.-Y. Yeng and H.-T. Chiu., *J. Cryst. Growth*, **2003**, *247*, 363-370.
2. F. Wuyou, Y. Haibin, C. Lianxia, Hari-Bala, L. Minghua and Z. Guangtian, *Colloids and surf. A: Physicochem. Eng. Aspects* **2006**, *289*, 47-52.
3. U. Dielbold, *Surf. Sci. Rep.*, **2003**, *48*, 53-229.
4. H. A. Al-Abadleh and V.H. Grassian, *Surf. Sci. Rep.*, **2003**, *52*, 63-161.
5. M. R. Hoffman, S.T. Martin, W. Choi and D.W. Bahnemann, *Chem. Rev.*, **1995**, *95(1)*, 69-96.
6. A. L. Linsebigler, G. Lu and J. T. Yates, *Chem. Rev.*, **1995**, *95(3)*, 735-758.
7. M. I. Litter, *Appl. Catal. B: Environ*, **1999**, *23*, 89-114.
8. K. Wilke and H.D. Breuer, *J. Photochem. Photobiol. A*, **1999**, *121(1)*, 49-53.
9. I. Justicia, G. Garcia, L. Vázquez, J. Santiso, P. Ordejón, G. Battiston, R. Gerbasi and A. Figueras, *Sensor and Actuator B: Chemical*, **2005**, *109*, 52-56.
10. A. Fujishima, T. N. Rao and D. A. Tryk, *J. Photochem. Photobiol. C: Photochem. Rev.*, **2000**, *1*, 1.
11. C. Chen, X. Li, W. Ma, J. Zhao, H. Hidaka and N. Serpone, *J. Phys. Chem. B*, **2002**, *106*, 318-324.
12. X. Liu, *Powder Technology*, **2012**, *224*, 287-290
13. N. Negishi and K. Takeuchi, *J. Sol-Gel Sci. Technol.*, **2001**, *22*, 23-31.
14. B. Souvereyns, K. Elen, C. De Dobbelaere, A. Kelchtermans, N. Peys, J. D'Haen, M. Mertens, S. Mullens, H. Van den Rul, V. Meynen, P. Cool, A. Hardy and M.K. Van Bael, *Chemical Engineering Journal*, **2013**, *223*, 135-144
15. J. Lützenkirchen, J. F. Boily, L. Lovgren, and S. Sjöberg, *Geochim. Cosmochim. Acta* **2002**, *66*, 3389-3396.

16. J. Lützenkirchen, *J. Colloid Interface Sci.*, **2005**, *290*, 489–497.
17. T. Ivanova, A. Harizanova, T. Koutzarova and B. Vertruyen; *Journal of Non-Crystalline Solids*, **2011**, *357*, 2840–2845.
18. V. G. Erkov, S. F. Devyatova, E. L. Molodsova, T. V. Malsteva and U. A. Yanovski, *Appl. Surf. Sci.*, **2000**, *166*, 51-56.
19. J.-Y. Zhang, I. W. Boyd, B. J. O’Sullivan, P.K. Hurley, P. V. Kelly and J. P.-. Sénateur, *J. Non-Cryst. Sol.*, **2002**, *303*, 134-138.
20. G. Hausinger, H. Schmelz and H. Knözinger, *Appl. Catal.*, **1988**, *39*, 267-283.
21. A. Ranga Rao and V. Dutta, *Sol. Energy Mater. and Sol. Cells*, **2007**, *9*, 1075-1080.
22. T. Yoko, K. Kamiya and K. Tanaka, *J. Mater. Sci.*, **1990**, *25*, 3922-3929.
23. E. Jr. Morgado, M.A.S. de Abreu, G.T. Moure, B.A. Marinkovic, P.M. Jardim and A.S. Araujo, *Chem. Mater.*, **2007**, *19 (4)*, 665–676.
24. H. Zou and Y.S. Lin, *Appl. Catal. A: General*, **2004**, *265*, 35–42.
25. S. G. Gregg and K. S.W. Sing, “Adsorption, Surface Area and Porosity 2<sup>nd</sup> Ed., Academic Press, London, **1982**.
26. M. Bouby, J. Lützenkirchen, K. Dardenne, T. Preocanin, M. A. Denecke, R. Klenze and H. Geckeis, *J. Colloid Interface Sci*, **2010**, *350*, 551-561.
27. T. Preocanin and N. Kallay, *Croat. Chem. Acta*, **2006**, *79 (1)*, 95-106.
28. F. Dumont, P. Verbeiren and C. Buess-Herman *Colloids and Surfaces*, **1999**, *A 154*, 149-156.
29. W. Piasecki, P. Zarzycki and R. Charnas, *Adsorption*, **2010**, *16*, 295–303.
30. J. Lyklema, *Chemical Physics Letters*, **2009**, *467*, 217–222.
31. W. Stumm “Chemistry of the solid-water interface: Processes at the mineral-water and particle-water interface in natural systems”, Wiley Interscience Pub., New York **1992**.
32. C.-P. Huang and W. Stumm, *J. Colloid Interface Sci*, **1973**, *43*, 409-420.
33. J.-Ph. Boisvert , A. Malgat , I. Pochard and C. Daneault. *Polymer*, **2002**, *43*, 141-148.
34. T. E. Payne, Davis, J. A, G.R. Lumpkin, R. Chisari and T. D. Waite, *Applied Clay Science*, **2004**, *26*, 151-162.
35. G.A. Waychunas, C.C. Fuller and J.A. Davis, *Geochimica et Cosmochimica Acta*, **2002**, *66*, 1119-1130.
36. A. Malgat, J.P. Boisvert and C. Daneault , *J. Colloid. Interface. Sci*, **2004**, *269*, 320-328
37. R.J. Hunter in « *Fundation of Colloid Science* »Volume 1, Ed. Clarendon Press Oxford, **1987**, pp. 379-391.
38. E. Ghenne, F. Dumont and C. Buess-Herman, *Colloids and Surfaces* **1998**, *131*, 63-67.
39. N. Kallay, S. Zalac, *J. Colloid. Interface. Sci*. **2000**, *230*, 1-11.